AN OVERVIEW OF THE NEURAL NETWORK BASED TECHNIQUE FOR MONITORING OF ROAD CONDITION VIA RECONSTRUCTED ROAD PROFILES

Harry M. Ngwangwa[1], P. Stephan Heyns[1], Kobus F. J. J. Labuschagne[2] and Grant K. Kululanga[3]

1. Dynamic Systems Group, Department of Mechanical and Aeronautical Engineering, University of Pretoria, 0002 Pretoria, South Africa
Tel: +27124204382; Fax: +27123625087
Email: harry.ngwangwa@tuks.co.za or hngwangwa@csir.co.za
2. Intelligent Systems and Traffic Management, Built Environment, CSIR, 0001 Pretoria, South Africa
3. Department of Civil Engineering, University of Malawi, The Polytechnic, Private Bag 303, Chichiri, Blantyre 3, Malawi

ABSTRACT

A healthy road transport system is essential for any country's social and economic development. It is generally observed that if road deterioration is allowed to increase, the economy will need significantly larger expenditures in subsequent years to keep the road maintenance backlog constant. This paper is part of a larger study whose main purpose is to investigate the dynamic behaviour of vehicles on the roads and how the observed behaviour can be effectively combined with other factors measured on the road and driver to assess the integrity of road and vehicle infrastructure. In this paper, vehicle vibration data are applied to an artificial neural network to reconstruct the corresponding road surface profiles. The results show that the technique is capable of reconstructing road profiles within an error margin of 45 percent while with careful control of principal error sources, the technique may achieve 20 percent error margin. This is considered to be reasonable enough for application to condition monitoring of unpaved roads servicing heavy vehicles.

Keywords:
artificial neural network, road condition monitoring, road profile reconstruction, vehicle dynamic modelling, vehicle vibration.

1. INTRODUCTION

The problems associated with safety, economy, and overall quality of road transportation are influenced by the characteristics of both roads and vehicles and by the manner in which these two systems interact. The vehicle-road interaction problem has been largely used as a platform for investigations into the mechanics of vehicle-induced road damage, road-induced vehicle damage and ride comfort. The nature of the interaction is also perceived to negatively affect the vehicle's fuel consumption and driver performance. Studies show that these problems increase with more roughness on the road surface (OECD Expert Group, 1994 & 1998; Cebon, 1999). Thus a critical issue has always been to avoid serious deterioration of road infrastructure by implementing a condition-triggered maintenance schedule.

Highway Design and Maintenance (HDM) model was developed to optimize the economic benefits given by road maintenance. However, HDM cannot be applied directly within any local operating conditions for the first time without some sort of calibration (Rohde, Zooste, Sadzik, Henning, 1998; Caroff, Freneat, Riviere, Spernol, 2001; Jain, Aggarwal, Parida, 2005). Secondly, HDM is largely viewed as World Bank tool for evaluating the viability of road maintenance, rehabilitation and construction projects, and as such, it might be largely used in situations where justification is required to solicit World Bank funds. Besides, HDM model still require road condition parameters obtained from good road inventory (Tsunokawa, Ul-Islam, 2007) often collected through visual inspections or using one of a limited number of instrumented vehicles. It is therefore necessary to develop alternative methods of assessing the integrity of roads.

In order to achieve that, it is necessary first to obtain a correct road surface profile. There are many methods reported in the literature for obtaining road profiles by direct measurements of the road itself (Sayers, Gillespie, Paterson, 1986; Cundill 1991; Sayers, Karamihas, 1998). However, Gonzalez, O'brien, Li, Cashell (2007) argue that such methods are expensive hence they present a numerical validation of a method for estimating road roughness using the accelerations obtained on the vehicle body and axles. The road roughness is expressed as a power spectral density (PSD) function according to International Standards Organisation (ISO) classification (ISO 8608, 1995). The recent developments in vehicle design where accelerometers are being mounted on chassis systems in order to improve suspension performance makes this technique relatively inexpensive.

This paper presents a numerical verification of a technique that is developed from earlier work by Hugo, Heyns, Thompson, Visser (2007). In their work, Hugo et al. (2007) developed a condition-triggered maintenance system for mine haul roads based on profile reconstruction. Their approach was based on inverting a multi-body dynamics model of the haul truck which was developed from extensive characterization of the truck. The haul road profile was then generated by applying responses measured on the truck to the inverse model. Gonzalez et al. (2007) adopted almost a similar approach with the exception that they employed a transform function which related the PSD function of the vehicle's accelerations to the PSD function of the road profile. Both approaches involve characterizing the system, formulating the system dynamic models, determining their inverses and applying the vehicle responses to the inverses. This could become onerous where vehicle manufacturers' data are not readily available and desired accuracies demand using more degrees-of-freedom and more expensive tyre models.

In order to avoid such problems, this work employs an artificial neural network (ANN) to reconstruct the road profile. Typically, the ANN is trained with vehicle responses (as input data) and road profiles (as target data) obtained from known road roughness classes on the ISO classification scale shown in Figure 1. Road roughness increases with the letters hence class A represents a very good road profile while class H represents badly deteriorated road. Taylor, Zongwane, Thompson, Visser (2001) and Thompson, Visser, Miller, Lowe (2003) used ANN to assist them in recognizing specific mine haul road defects qualitatively. Thompson et al. (2003) realize need for an ability to analyse, recognize and interpret various forms of the same defect signature and need for use of multi-sensor data to isolate faults from different sources. This paper lays a foundation to such work via a numerical analysis of the capabilities of the ANN to reconstruct road profiles and their attendant road defects.

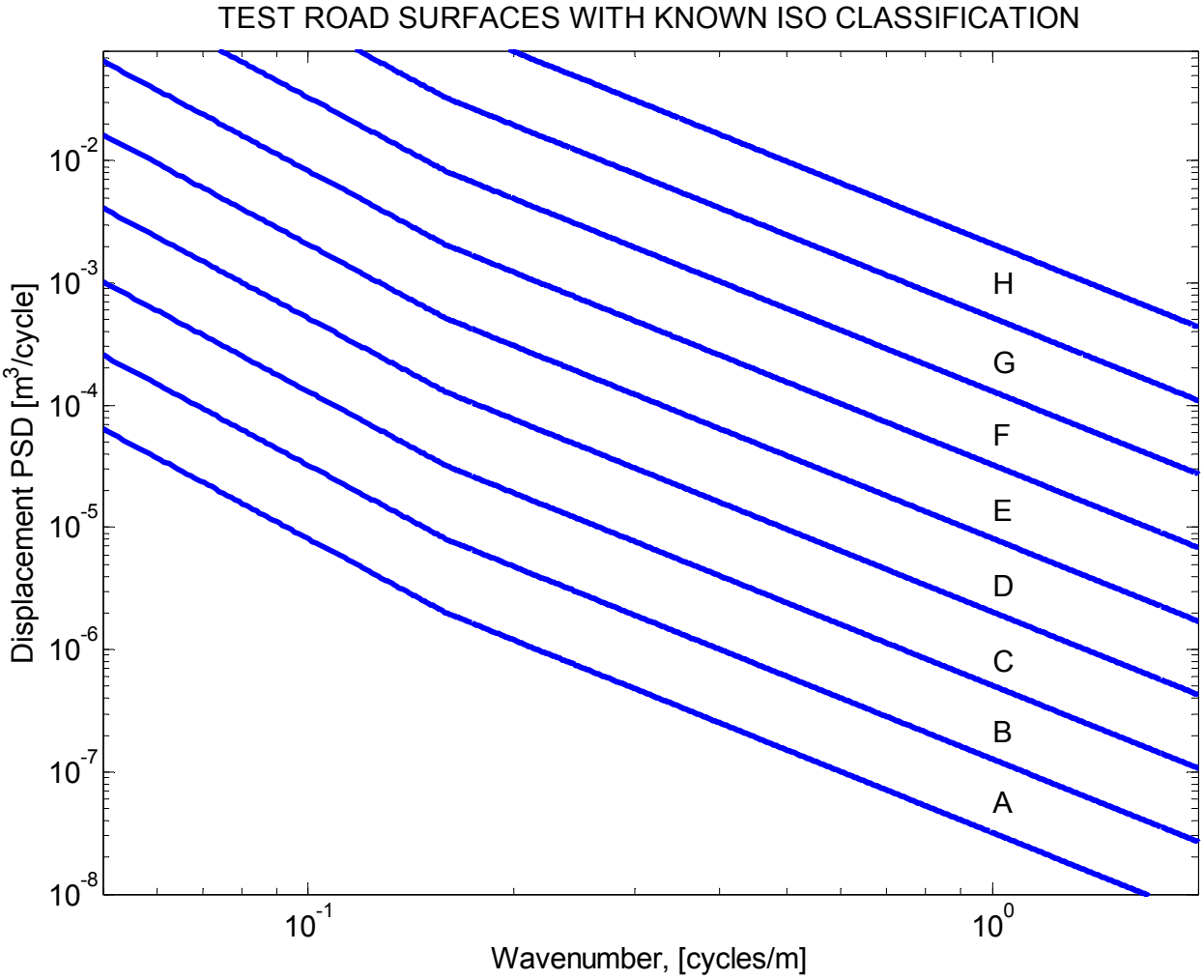

Figure 1 Road roughness classification according to ISO 8608 1995(E)

In this paper, the road roughness classification is done using both PSD and the widely used roughness indicator the International Roughness Index (IRI). IRI helps to determine overall road condition, road serviceability level and prioritizing maintenance while PSD detects presence of road dependent faults and the existence of any periodic defects in the road profile. This is necessary since IRI is merely a statistic that summarizes the roughness qualities of a road network that impacts vehicle response and cannot in itself reveal existence of destructive frequencies in the road profiles.

This paper is structured as follows. Section 2 describes, via a simple diagram, the road profile reconstruction and roughness classification procedure. Relevant theory is covered under section 3, comprising vehicle modelling, generation of road surface topography, calculation of IRI and road profile reconstruction using ANN. Section 4 presents the two numerical examples used to verify the technique. The discussions of the results are presented separately in Section 5. The work is concluded in Section 6.

2. PROPOSED METHOD OF ROAD CONDITION MONITORING

The proposed technique is outlined in Figure 2. The technique begins by computing road profiles corresponding to each roughness class as given in Figure 1. The resulting road profiles are applied to a vehicle model which calculates vehicle responses. These vehicle responses and their corresponding road profiles are processed and used to create and

train the ANN. The decision block examines correlation between the outputs from ANN and the processed road profiles. It is important to note that the correlation is necessary during network creation and training.

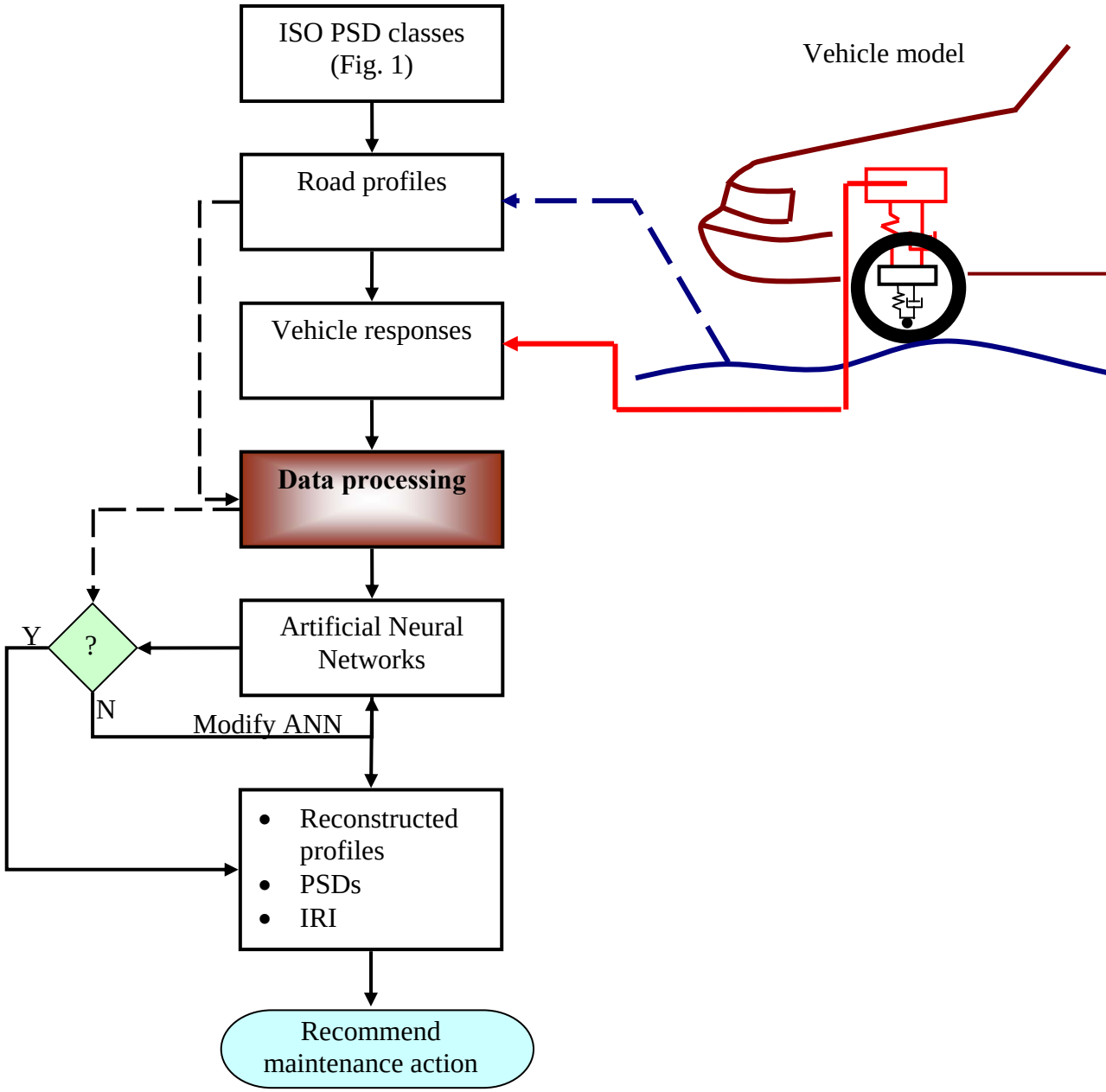

Figure 2 Layout of the simplified reconstruction and roughness classification procedure

During testing, different road profiles from the ones used in training the ANN are generated and applied to the vehicle model to obtain corresponding vehicle displacement responses. These displacement responses are used to simulate the network while their corresponding road profiles (if available as it is here) are merely used in verifying the accuracy of the reconstructed road profiles. The test data are applied to similar data processing system as the training data before they could be used in simulating the ANN. Typically that involves low pass filtering and mapping the data onto the normalized coordinate plane since most implementations of ANN perform better with normalized data.

The ANN produces reconstructed road profiles, displacement PSD and IRI. These results may be sent directly to a real-time road maintenance management system to trigger maintenance and/or may be stored in a databank for access by any interest groups. The reconstructed profile may be very useful in locating the damage and identifying road sections that require urgent attention.

The class of road roughness, as obtained from the displacement PSD and IRI may be helpful where the conditions for various road networks are required and there is need for maintenance prioritization especially on more severely damaged road networks. Displacement PSD can further be used to investigate offending frequencies (if any) and/or transmitted dynamic forces to the cab, pay load and road surface.

3. THEORY

1.1 Vehicle Modelling

The mathematical equations used for representing vehicle-road interaction may be written in matrix form as follows (Gillespie, 1992; Cebon, 1999):

$$\mathbf{M}\ddot{\mathbf{z}} + \mathbf{C}\dot{\mathbf{z}} + \mathbf{K}\mathbf{z} = \mathbf{f} \quad (1)$$

where **M** is a matrix representing vehicle body mass; **C** is a matrix of vehicle damping

K is the stiffness matrix of the vehicle; **z** is a vector of vehicle dynamic responses, and **f** is a vector of force inputs acting on the vehicle.

A quarter-car model shown in Figure 3 is commonly used to investigate dynamics of heavy vehicles without trailers. In steady-state vibration the dynamic behaviour of the model may be determined by (Gillespie, 1992),

$$M_s\ddot{z}_s + C_s\dot{z}_s + K_s z_s = F_b + C_s\dot{z}_{us} + K_s z_{us} \quad (2)$$

$$M_{us}\ddot{z}_{us} + \left(C_s + C_t\right)\dot{z}_{us} + \left(K_s + K_t\right)z_{us} = F_w + C_s\dot{z}_s + C_t\dot{z}_r + K_s z_s + K_t z_r \quad (3)$$

However, as an initial investigation, the study assumes that tyre non-uniformities and driveline inputs are limited to minimal levels so that they may not influence the final sprung mass responses as significantly as road roughness. This assumption is fair considering the current state of wheel balancing technologies and a general awareness in ride quality. Tire non-uniformities that would cause similar vibrations to the sprung mass as road unevenness can be easily picked up during any vehicle service. Similarly, most vehicle vibrations caused by driveline inputs may be detected in standby mode and can easily be filtered out during data processing.

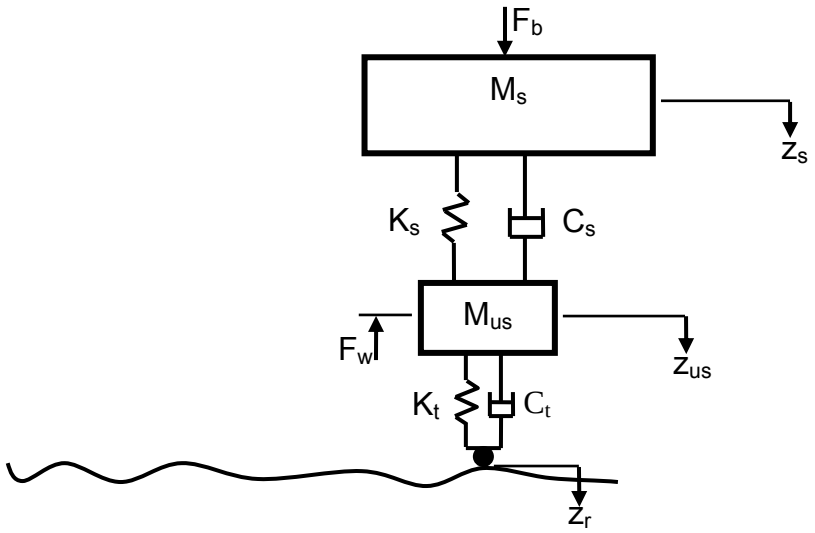

Figure 3 Quarter-car model excited by on-board forces (F_b), wheel non-uniformity (F_w) and road roughness (z_r)

3.2 Road Roughness Classification

The International Organization for Standardization (ISO) proposed a road roughness classification based on road displacement PSD (ISO 8608, 1995). The classification identifies eight road roughness levels ranging from Class A to Class H in increasing order of roughness. In the ISO classification, the relationships between the displacement PSD and the spatial frequency for different classes of road roughness may be approximated by (ISO 8608, 1995; Cebon, 1999).

$$S_u(\kappa) = \begin{cases} S_u(\kappa)\left(\dfrac{\kappa}{\kappa_0}\right)^{-n_1} & \dfrac{\kappa}{\kappa_0} \le 1 \\ S_u(\kappa_0)\left(\dfrac{\kappa}{\kappa_0}\right)^{-n_2} & \dfrac{\kappa}{\kappa_0} > 1 \end{cases} \qquad (4)$$

where $S_u(\kappa)$ is the displacement spectral density, expressed in m^3/cycle, κ is the wavenumber expressed in cycles/m, $S_u(\kappa_0)$ is the displacement spectral density at κ_0. (Values >128 m^3/cycle for poor/very poor roads) κ_0 is the datum or cut-off wavenumber.

The constants n_1, n_2 and κ_0 being equal to 3.0, 2.25 and 1/(2π) cycles m^{-1}, respectively.

The spectral density as given in (4) is usually calculated from measurement of surface roughness described by heights of equally spaced points along the road. However, in the absence of such measurements, pseudo-random profiles can be generated to fit those spectral densities. Cebon (1999) presents a formula for generating a single-wheel track random profile as,

$$z_r^{(1)} = \sum_{k=0}^{N-1} \sqrt{S_k}\, e^{i\left(\theta_k^{(1)} + \frac{2\pi kr}{N}\right)}, \qquad r = 0,1,2,\ldots(N-1) \qquad (5)$$

where $S_k = (2\pi/N\Delta)S_{11}(\gamma k)$, and $S_{11}(\gamma k)$ is the target spectral density, $\gamma k = 2\pi k/N\Delta$ is wavenumber in rad m^{-1}, Δ is the distance interval between successive ordinates of the surface profile and $\theta_k^{(1)}$ is a set of independent random phase angles uniformly distributed between 0 and 2π.

3.3 Calculation of IRI

International Roughness Index (IRI) is a standardized roughness measurement related to those obtained by the response-type road roughness measurement systems usually expressed in m per km or mm per m (Sayers et al., 1986). IRI is computed from a quarter-car simulation in which a ratio of the accumulated suspension motion of a vehicle is divided by the distance travelled by the vehicle at a standard velocity of 22.2 m s^{-1} during the test. It is a characteristic of the longitudinal road profile and therefore requires the availability of the road profile itself.

A scale for IRI covers roughness descriptions for airport runways through rough unpaved roads. Each type of track (whether airport runway, paved or unpaved road) has its own range on the IRI scale most of which overlap. However, most practical road ways can be represented between 0 and 16 m per km. Unpaved roads emerge from IRI values of around 3 m per km.

The calculation of IRI is accomplished by computing four variables as functions of the measured profile. The IRI statistic is the average of rectified slope (RS) variable over the entire length of the road under test (Sayers et al., 1986).

$$IRI = \frac{1}{N-1}\sum_{n=2}^{N} RS_n \qquad (6)$$

where N is the total number of elevation points in the road profile.

3.4 Road profile reconstruction using ANN

The problem of reconstructing the profile from given sets of vehicle responses is treated here as an inverse problem which is solved by ANN. Neural networks are composed of simple elements operating in parallel. The elements are inspired by biological nervous systems. As in nature, the network function is determined largely by the connections between elements.Figure 4 shows a generalized layout of a single-layer artificial neural network. Typically, neural networks work by adjusting the values of weights **w** and biases **b**, a process which is referred to as a learning rule or training algorithm.

In this work, a back-propagation network with a Levenberg-Marquardt training function is used. The Levenberg-Marquardt algorithm was designed to approach second-order training speed without having to compute the Hessian matrix (Hagan, Menhaj,1994; Mathworks Inc., 2007). The Levenberg-Marquardt algorithm adjusts the weights by using the following equation (Bishop, 1995).

$$\mathbf{w}_{new} = \mathbf{w}_{old} + \left(\mathbf{J}^T\mathbf{J} + \lambda\mathbf{I}\right)^{-1}\mathbf{J}^T\boldsymbol{\varepsilon}(\mathbf{w}_{old}) \qquad (7)$$

where **I** is the identity matrix, $\boldsymbol{\varepsilon}(\mathbf{w}_{old})$ is an error vector at the current point, $\mathbf{w}_{new}$ is the weight at the next point in the training procedure, **J** is the Jacobian matrix given by the partial derivative $\partial\boldsymbol{\varepsilon}(\mathbf{w}_{old})/\partial\mathbf{w}_{old}$ and λ is a parameter that governs the step size. The value of λ varies during network training.

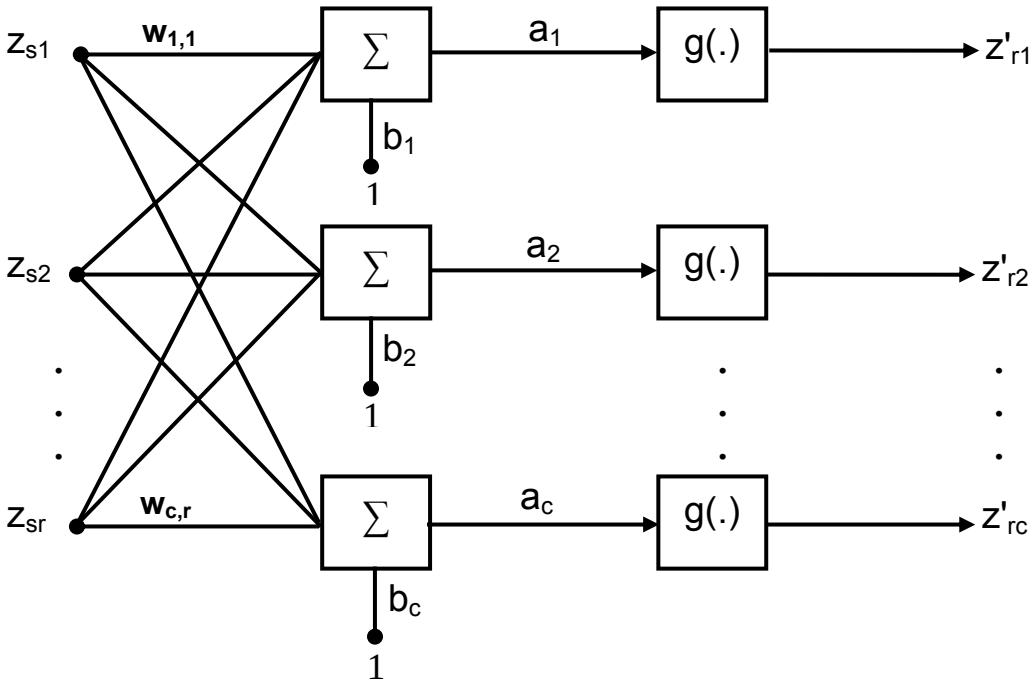

Figure 4 Generalized layout of a single-layer neural network with r inputs and c outputs

A nonlinear autoregressive with exogenous inputs (NARX) neural network is used to approximate the desired road profiles. It works in such a way that the next value of the output z'r is regressed on its previous values and previous values of an independent (exogenous) input signal zs. Thus the network output may be given by Equation (8) (Mathworks Inc., 2007).

$$z'_{rk} = f\left(z'_{rk}(t-1), z'_{rk}(t-2), ..., z'_{rk}(t-n_{z'_{rk}}), z_{sk}(t-1), z_{sk}(t-2), ..., z_{sk}(t-n_{z_{sk}})\right) \qquad (8)$$

The NARX network is recurrent dynamic, with feedback connections enclosing several layers (Mathworks Inc., 2007).

4. NUMERICAL EXAMPLES

The methodology is verified via a quarter-car model having the following physical properties as used in reference (Cebon, 1999): Mass of sprung mass, M_s = 8900 kg; Mass of unsprung mass, M_{us} = 1100 kg; Shock spring stiffness, K_s = 2 MN m^{-1}; Tire stiffness, K_t = 3.5 MN m^{-1}; and Shock damping constant, C_s = 40 kN s m^{-1}. It is assumed that tire damping, C_t is negligible and that the vehicle is driven at an average speed of 80 km h^{-1} (approximately 22.2 m s^{-1}). Thus the system's equation of motion at the sprung mass is similar to (2) while that at the unsprung mass can be modified as:

$$M_{us}\ddot{z}_{us} + C_s\dot{z}_{us} + \left(K_s + K_t\right)z_{us} = F_w + C_s\dot{z}_s + K_s z_s + K_t z_r \qquad (9)$$

The vehicle model has sprung mass and unsprung mass natural frequencies of 1.98 and 11.3 Hz, respectively. In order to capture the prominent frequencies, road profiles were generated using wave number range between 0.01 and 2 cycles m-1. This corresponds to frequencies between 0.22 and 44 Hz. Inclusion of higher frequencies than 44 Hz for the system under study is simply extravagant since the response gain due to road roughness

input at such frequencies is negligible.

Thereafter, road surface profiles z_r corresponding to each class boundary shown as dashed lines in Figure 5, are generated using Equation (5). The resulting road displacement inputs are applied to the quarter-car model to calculate vehicle displacement responses, z_s. The vehicle responses are used as inputs while the surface profiles as targets for training the ANN. Thus the training data typically covers the entire range of surface roughness (from Class A to Class H). This is to make the ANN adapt well to the vector space covered by the roughness classes.

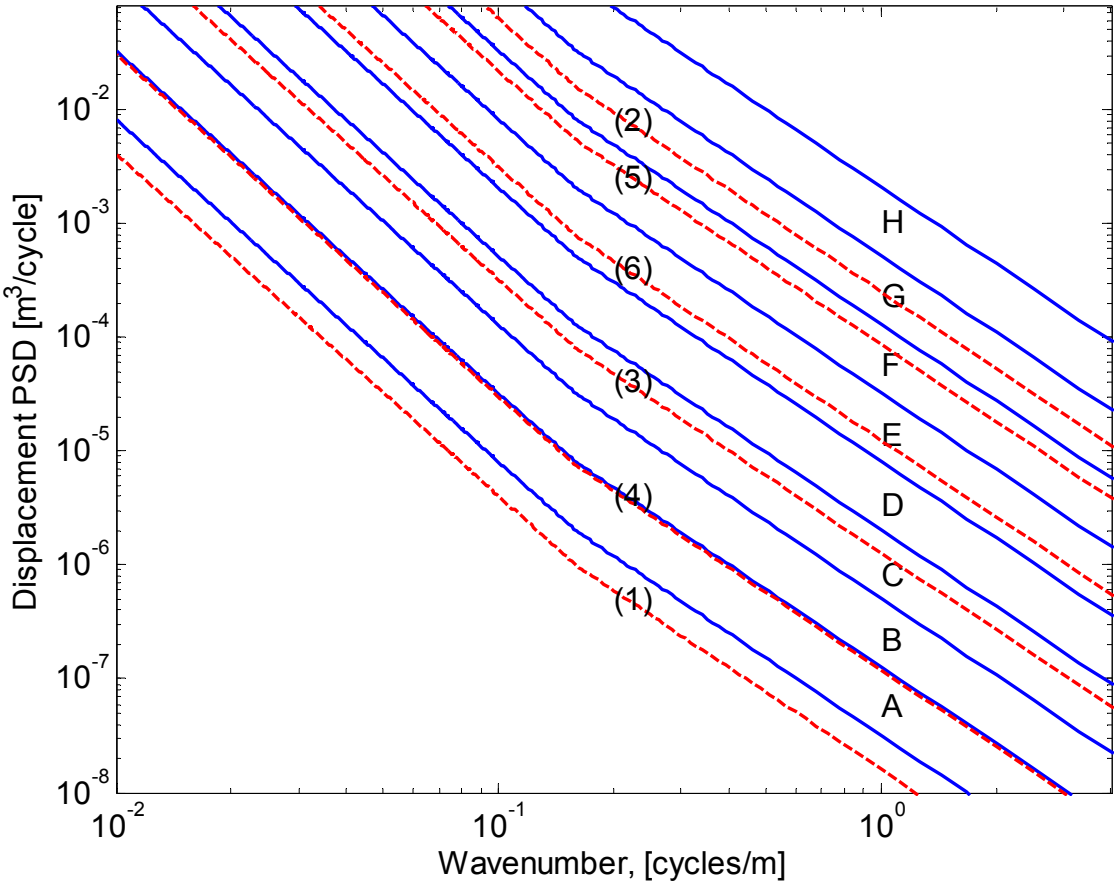

Figure 5 Road surfaces used in the test numbered according to testing sequence

A two layer NARX network with ten tan-sigmoid neurons in its hidden layer and one linear neuron in its output layer was chosen for the simulation. It uses the Levenberg-Marquardt algorithm as the training function owing to its superior performance in regression problems such as this one.

Two case studies are presented in this work. The first case study involves reconstruction and identification of the profiles per se, while the second study deals with the reconstruction of emerging road surface defects such as potholes, humps or ditch-hump. In the first study, we apply the road displacement PSD, shown in Figure 5 as solid lines, to the quarter-car model. The calculated vehicle responses are used to simulate the ANN for reconstruction of the road profiles. The numbers on the road displacement PSD represent the sequence in which the tests are performed.

In the second case study, we place two surface defects of known geometry along the road.

The road roughness classes, in this case, are only known in terms of the underlying roughness. The purpose of the case study is to demonstrate that the technique can reconstruct the road surface defects and establish expected accuracies.

5. RESULTS AND DISCUSSIONS

5.1 First case study: Identifying plain road roughness profiles

The results for the first case are displayed in **Error! Reference source not found.** The plots generally show good fit between the reconstructed and actual road profiles for all test roads though with varying degrees of accuracy as shown by the percent error plot in Figure 7. These plots show that the most accuracy is obtained in test profile (4) while test profiles (1) and (2) give the least accuracy. Inspection of Figure 5 reveals that the trend is related to the proximity of the PSD curve to any class boundary. However, that is a simple algorithmic anomaly that can easily be rectified by generating more training vectors within any particular class.

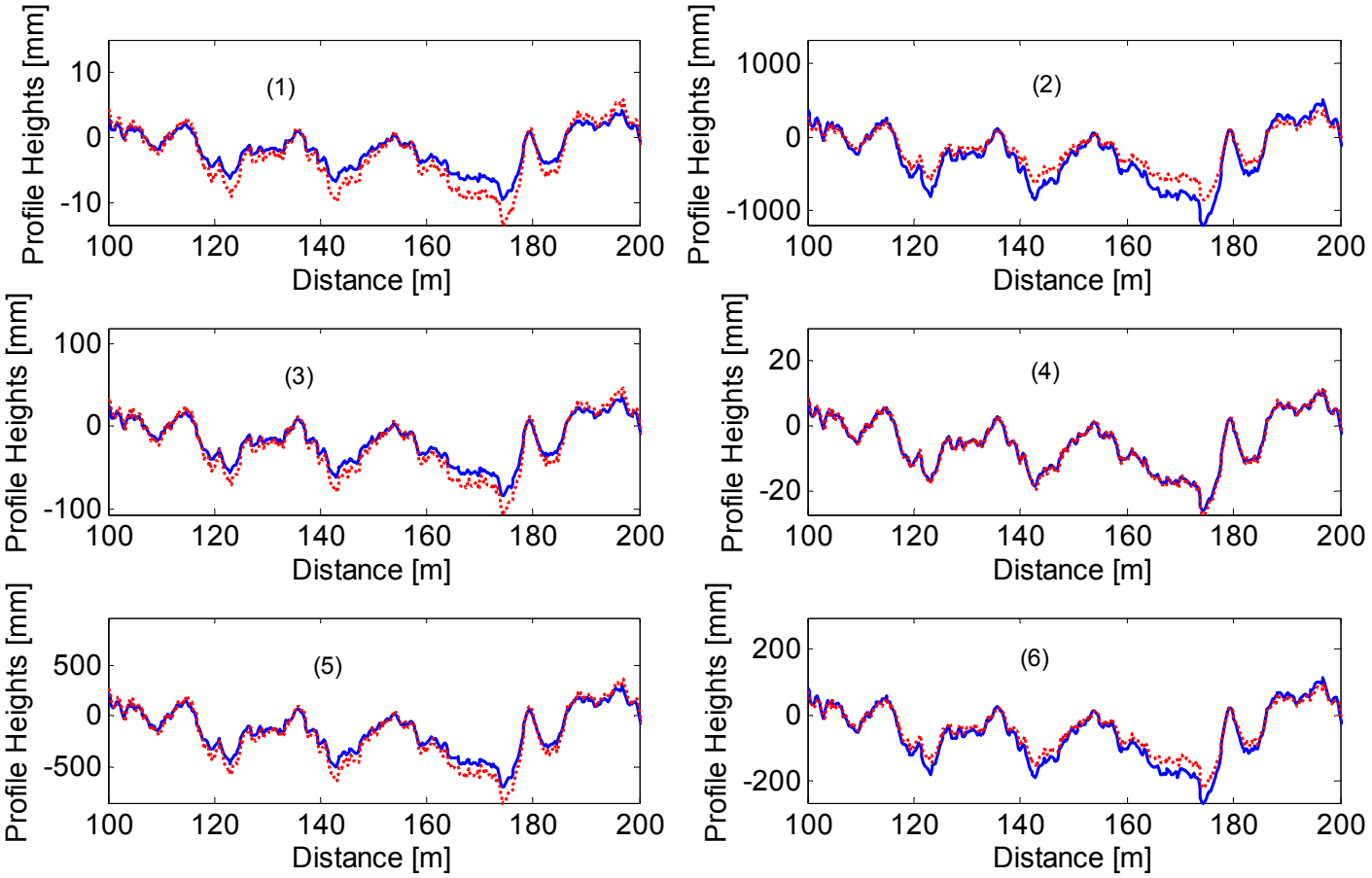

Figure 6 Reconstructed profiles (dotted red) plotted over Actual profiles (solid blue)

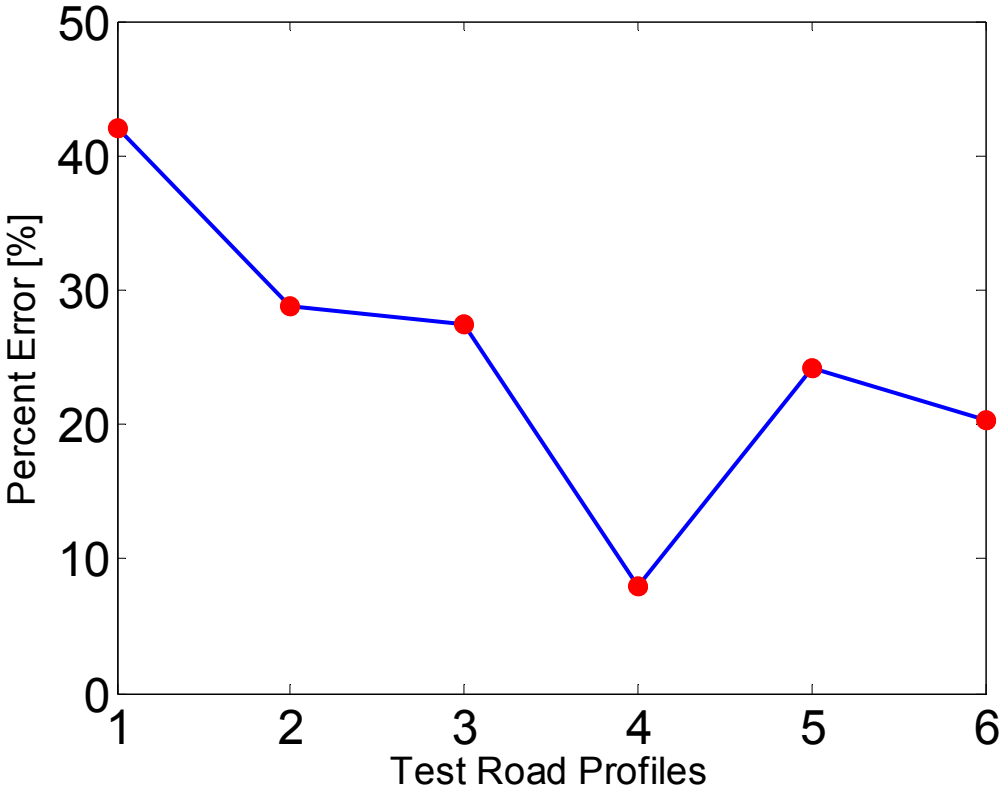

Figure 7 Errors between target and reconstructed road surface profile

In Figure 8 (a) profile reconstruction errors are calculated at various displacement PSD from 0.5 to 8 m^3 $cycle^{-1}$, typically from under the lower boundary up to the upper boundary of class A while in Figure 8 (b), the plot spans classes E and F. In both plots the network shows that errors diminish towards the class boundaries. Specifically, the plots show that the reconstructed profile falls within a 20 percent error margin for 25 percent proximity to the class boundary displacement PSD. In higher classes, the errors remain below 35 % as depicted by Figure 8 (b). However, correlation values are still above 99.9 % for all displacement PSD.

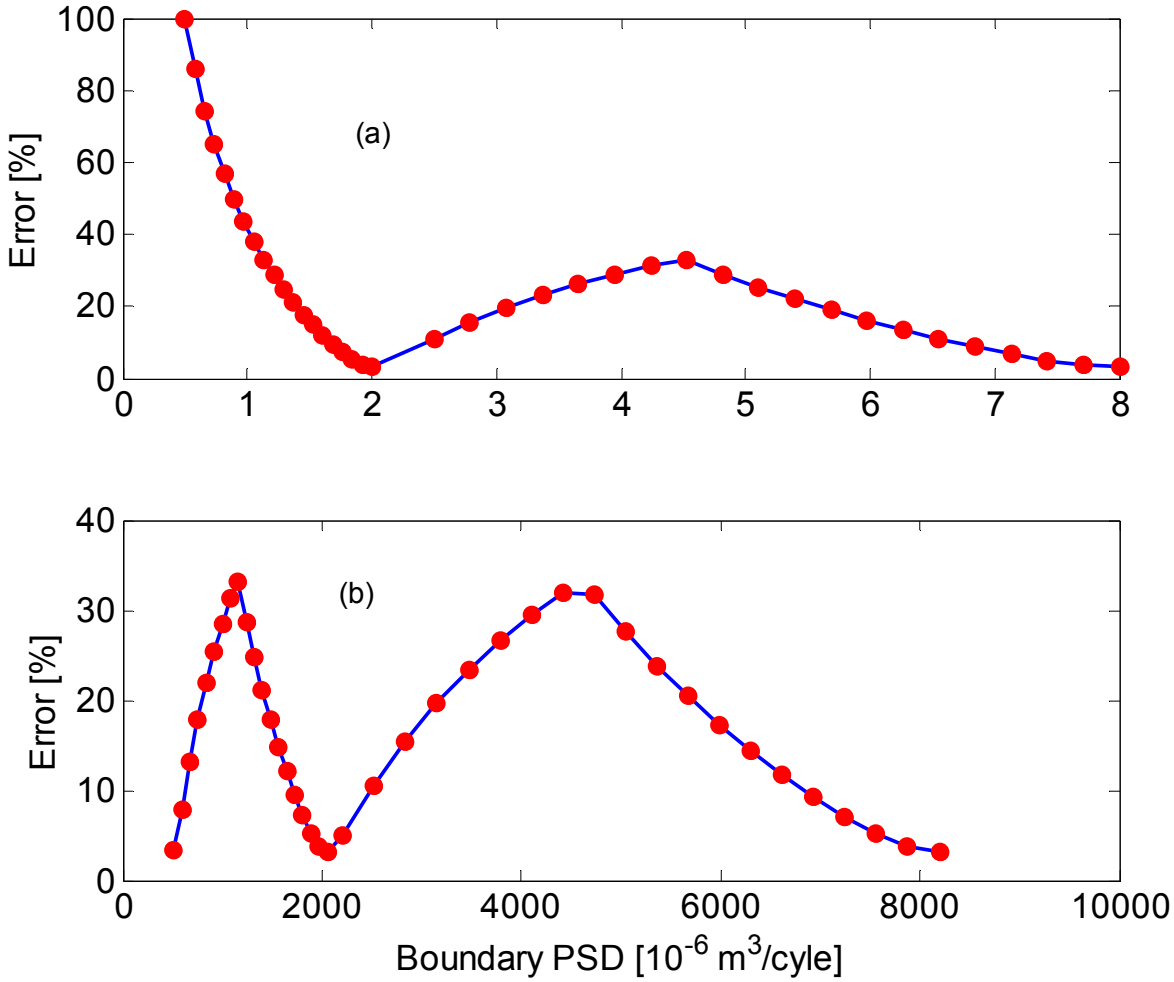

Figure 8 PSD proximity error around a displacement PSD in (a) class A (b) class E and F

5.2 Second case study: Identifying road roughness profiles containing prominent defects

The second case study investigates the ability of the technique to reconstruct and classify a road segment having local defects like ditches, humps or their combination. Firstly, a 5 m long 10 mm deep half-sine ditch is located between 210 and 215 m along roads of varying roughness classes. The vehicle is assumed to travel along the road at a constant speed of 22.2 m s^{-1}.

The results in Figure 9 and Figure 10 show the reconstructed defects in test roads (1) and (4). The sizes of the defects make them more noticeable in these two test roads than in the others. The defects are accurately located between 210 and 215 m, and between 470 and 475 m from start. The network accurately reconstructs both the half-sine ditch and the full-sine ditch-hump. This may enable detection and location of localised defects.

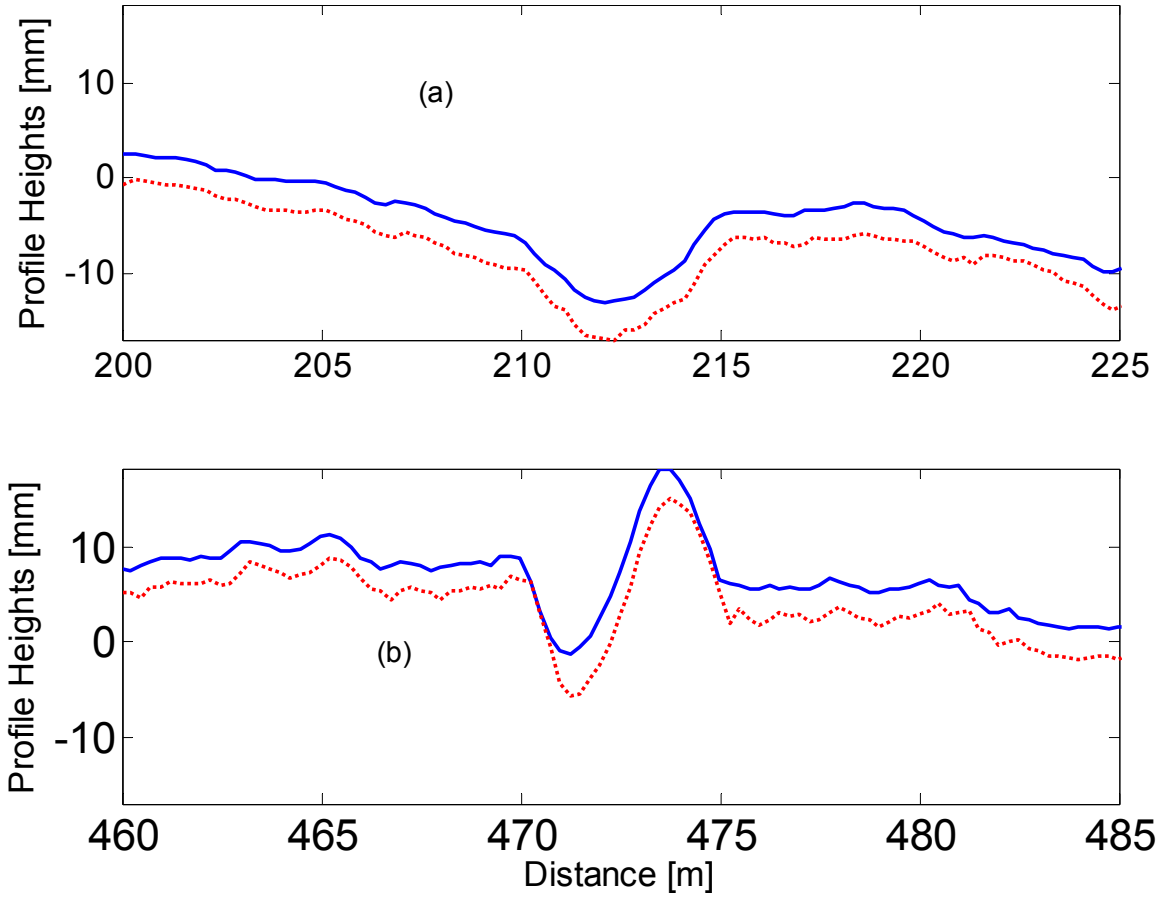

Figure 9 Defect reconstruction in test road (1) (a) ditch between 210 and 215 m (b) ditch-hump between 470 and 475 m

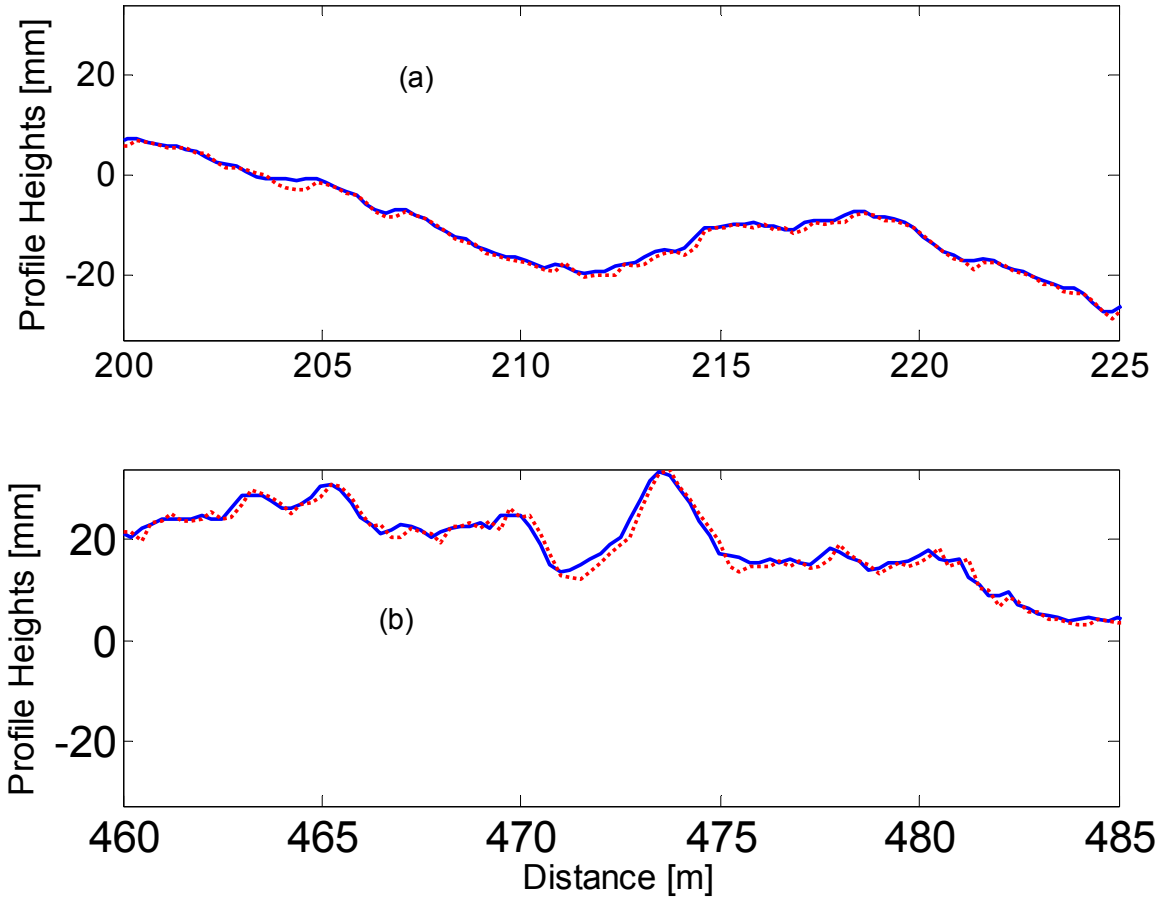

Figure 10 Defect reconstruction in test road (4) (a) ditch between 210 and 215 m (b) ditch-hump between 470 and 475 m

Accurate defect reconstruction, like in Figure 10, may be used to estimate longitudinal dimensions of the defect though its exact geometry in the transverse direction may require more data. It is envisaged that use of digitized road images may assist in achieving that goal. Although such data might not be enough for a final road maintenance decision, the data may still be useful in quantifying road damage.

5.3 Road roughness classification: combined use of displacement PSD – IRI

Road roughness classification is performed on the previously reconstructed profiles to examine how they compare with the actual classifications. In Table 1, we tabulate actual road classifications with classifications as obtained from computations of the roughness indicator IRI. It is noted that IRI classifies correctly four out of six roads. At the bottom of the table the calculated values of IRI for each test profile are given and they confirm the classification when compared with the IRI class boundaries at the top.

Figure 11 shows the computed PSD functions of the first three test roads only for clarity. The plotted results somewhat agree with the IRI classifications in Table 1. Since the added defects were constructed from periodic functions, it is observed that the PSD for test road (1) has a slight dimple in the middle around the affected frequencies. This is the added advantage of using the PSD with IRI classification. However, PSD classification may not be easy to use especially at upper end of the classes where lines that are numerically distinct by IRI measure may look superimposed on the plot. It can be a poorer tool for comparing roughness levels of different test roads within the same class of damage or even belonging to neighbouring classes.

Table 1 Test road profile data and their classifications

ISO CLASSES WITH THEIR IRI EQUIVALENTS								
ISO	A	B	C	D	E	F	G	H
IRI	0.3 – 0.6	0.6 – 1.2	1.2 – 2.4	2.4 – 4.7	4.7 – 9.5	9.5 – 19.0	19 – 37.8	37.8 – 76.0
TEST ROAD	CLASSIFICATION: A = ACTUAL, I = IRI							
(1)	A, I							
(2)							A, I	
(3)			A	I				
(4)	A, I							
(5)						A	I	
(6)					A,I			
CALCULATED IRI VALUES								
	(1)	(2)	(3)	(4)	(5)	(6)		
	0.3526	20.8378	2.8069	0.5290	20.8939	5.2740		

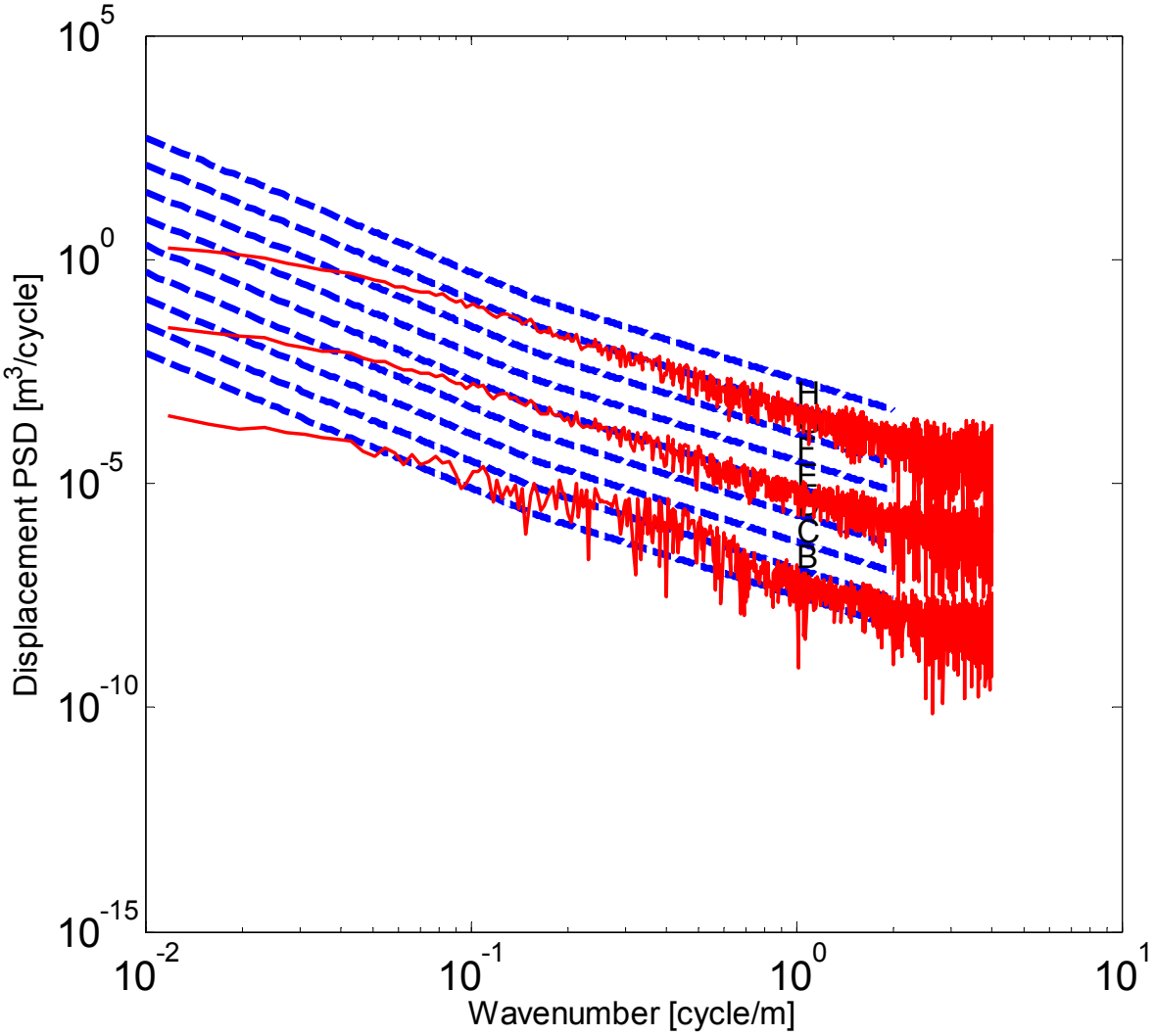

Figure 11 Road displacement PSD functions of test roads (1), (2) & (3) plotted over the ISO PSDs

Finally, the technique was simulated with data contaminated by different levels of noise from 0 to 50 percent of the vehicle's RMS response value. The errors shown in Figure 12 were averaged over ten numerical tests for each noise level. However if errors from other sources may be kept below 15 %, noise levels might not be permitted to exceed 4 % of the profile RMS values if a 20 % error margin is desired. This goal can be achieved by implementation of appropriate filters.

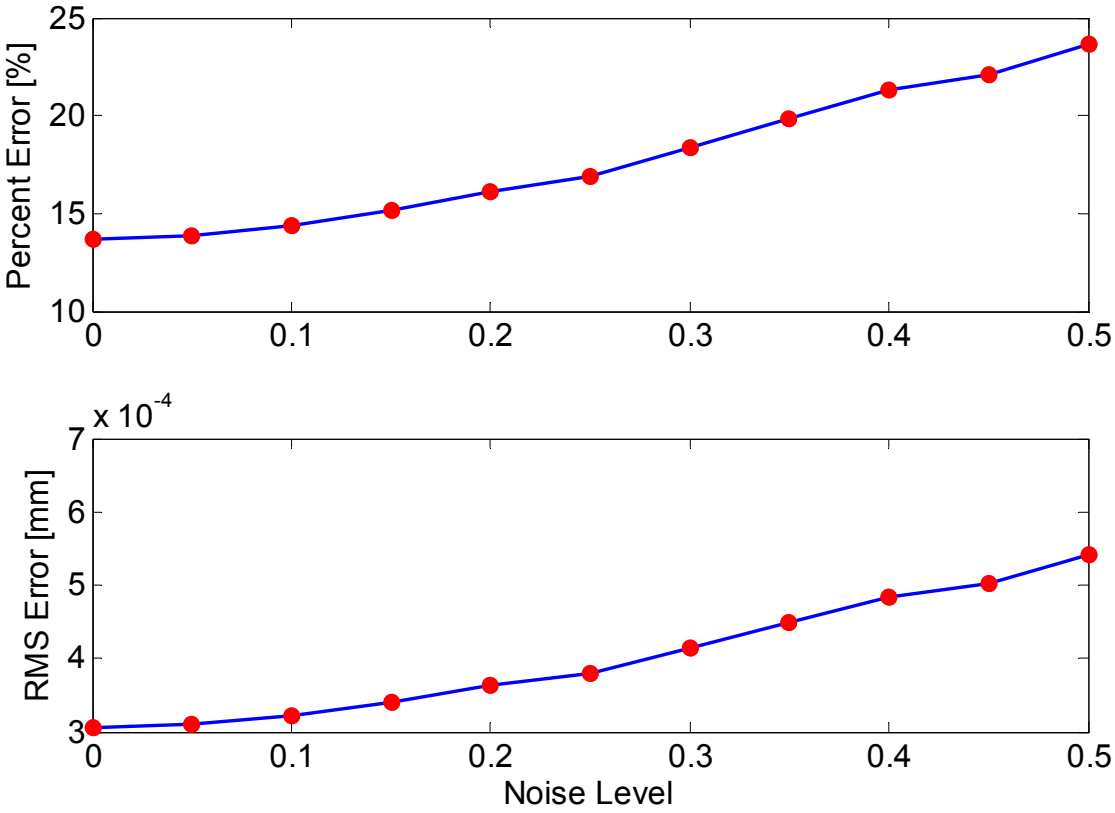

Figure 12 Errors in the presence of noise averaged for 10 tests

6. CONCLUSIONS

The technique for assessing road condition through reconstruction of road profiles and road defects is numerically verified. It avoids the use of expensive system characterization by employing ANN in the reconstruction procedure. It is shown that with enough training data and careful noise control, the technique has potential to achieve accuracies within 20 percent error.

The technique draws its advantages from the combined use of IRI, PSD and road profiles. IRI assists in determining roughness classification, road serviceability and maintenance prioritization while PSD assesses existence of periodic faults which might be very detrimental to vehicle frame and the road profiles can assist in pinpointing deteriorated sections. The knowledge of the geometry and geographical location of the road defect may assist in making a better maintenance decision.

The availability of vehicles mounted with accelerometers and global positioning systems (GPS) also makes this work worthwhile. Thus the work has potential for development of inexpensive real-time condition-triggered maintenance systems. The technique can provide a way of acquiring relevant road condition data useful for making fast road

management decisions or to act as input into more comprehensive maintenance models like the HDM.

7. REFERENCES

[1] Bishop CM (1995). *Neural networks for pattern recognition*, Oxford University Press, Oxford.

[2] Caroff G, Freneat E, Riviere N, Spernol A (2001). The Calibration of the HDM-4 Model in Eastern Europe, Routes/Roads, *World Roads Association* 311 47–58.

[3] Cebon D (1999). Handbook of vehicle-road interaction. Swets & Zeitlinger Publishers Lisse.

[4] Cundill MA (1991). The Merlin low-cost road roughness measuring machine, Transport and Road Research Laboratory, Digest of Research Report 301, Crowthorne, Berskshire.

[5] Gillespie T D (1992). Fundamentals of vehicle dynamics. Society of Automotive Engineers, Inc., Warrendale.

[6] Gonzalez A, O'brien EJ, Li YY, Cashell K (2007). The use of acceleration measurements to estimate road roughness. Vehicle System Dynamics 46:6 483 – 499.

[7] Hagan MT, Menhaj MB (1994). Training feedforward networks with the Marquardt algorithm, IEEE Transactions on Neural Networks, 5:6 989-993.

[8] Hugo D, Heyns SP, Thompson RJ, Visser AT (2007). Condition-triggered maintenance for mine haul roads with reconstructed –vehicle response to haul road defects. Transportation Research Record 2:1989 254 – 260.

[9] International Organization for Standardization ISO 8608: (1995(E)), Mechanical vibration - Road surface profiles – Reporting of measured data.

[10] Jain SS, Aggarwal S, Parida M (2005). HDM-4 Pavement Deterioration Models for Indian National Highway Network, *Journal of Transportation Engineering* 131 623–631.

[11] Mathworks Inc., (2007). Help Tutorial: Neural Networks Toolbox.

[12] OECD Scientific Expert Group IR6, Dynamic interaction between vehicles and infrastructure experiment, (DIVINE), 1998, Technical Report, http://www.oecd.org/dataoecd/8/57/2754406.pdf

[13] OECD Road Transport Research, Road maintenance and rehabilitation: funding and allocation strategies, 1994, Technical Report, http://www.oecd.org/dataoecd/0/50/1616608.pdf

[14] Rohde GT, Zooste F, Sadzik E, Henning T, (1998), The calibration and use of HDM-IV performance models in a pavement management system, *Proceedings of the* Fourth *International Conference on Managing Pavements,* Durban.

[15] Sayers MW, Karamihas SM, (Sept 1998). The little book of profiling: Information about measuring and interpreting road profiles, http://www.umtri.umich.edu/erd/roughness/. Accessed June 2007.

[16] Sayers, MW, Gillespie, TD, and Paterson, WDO (1986). Guidelines for Conducting and Calibrating: Road Roughness Measurements, World Bank Technical Paper Number 46, The World Bank, Washington, D.C., U.S.A.

http://www.romdas.com/romdascd/info/other/roughness/guidelines.pdf Accessed June 2007

[17] Taylor J, Zongwane B, Thompson RJ, Visser AT, (2001). The proposed implementation of a condition-triggered haul road maintenance system at Jwaneng mine. Sixth International Symposium on Mine Mechanization and Automation, South African Institute of Mining and Metallurgy.

[18] Thompson RJ, Visser AT, Miller RE, Lowe NT, (2003). Development of real-time mine road maintenance management system using haul truck and road vibration signature analysis, *Transportation Research Record* 1819A 305 – 312.

[19] Tsunokawa K, Ul-Islam R, (2007). Pitfalls of HDM-4 strategy analysis, *International Journal of Pavement Engineering* 8 67–77.